

Present-day vertical crustal deformations in West Greenland from repeated GPS observations

R. Dietrich, A. Rülke and M. Scheinert

TU Dresden, Institut für Planetare Geodäsie, 01062 Dresden, Germany. E-mail: dietrich@ipg.geo.tu-dresden.de

Accepted 2005 July 28. Received 2005 July 4; in original form 2005 January 17

SUMMARY

A GPS network, consisting of 10 sites, was established in the ice-free area of West Greenland and was observed for the first time in 1995. In 2002 a complete re-observation was carried out. These repeated GPS observations served as a basis for the determination of vertical crustal deformations. The data analysis was performed using the Bernese Software version 5.0. For the central site Kangerlussuaq a negative uplift rate (subsidence) of (-3.1 ± 1.1) mm yr⁻¹ was obtained, related to the reference frame IGB00. The regional pattern is characterized by an east–west gradient of up to 4 mm yr⁻¹ between the outer coast and the subsiding area along the present ice margin, which can be explained to a great extent as a result of the late Holocene re-advance of the Greenland ice sheet. Relative sea-level changes could be calculated taking the present eustatic sea-level rise into account. The present-day sea level rises at the outer coast between Maniitsoq and Paamiut, and in the large fjords with increasing rates of more than 4 mm yr⁻¹ in their innermost parts. These findings are in agreement with the general picture obtained from geomorphological and archaeological research. For Sisimiut and the Disko Bay area the present sea-level change is almost zero, whereas the crustal uplift rate for Ilulissat was observed to be 1.6 mm yr⁻¹. We conclude that this present vertical uplift rate in Ilulissat is affected by the retreat of the ice margin during the last 150 yr and the present negative mass balance of the Jakobshavn Isbræ and its drainage basin.

Key words: geodesy, geodynamics, glacial rebound, GPS, Greenland, sea level.

1 INTRODUCTION

Recent satellite gravity missions, especially the GRACE mission, allow to detect mass changes in the earth's system with unprecedented accuracy. This includes the detection of mass changes of large ice sheets as well as mass changes of the solid earth caused by post-glacial rebound. In order to discriminate between ice and solid earth contributions for a region like Greenland, additional information is necessary. This information originates from observations of different type, from models predicting recent crustal deformations of the earth based on an ice load history model or from a combination of both.

Whereas for formerly glaciated areas on the northern hemisphere like Fennoscandia, a variety of different observations on recent vertical crustal movements like tide gauge data (e.g. Ekman 1993), repeated gravity lines (e.g. Ekman & Mäkinen 1996) and GPS observations (e.g. Mäkinen *et al.* 2003; Scherneck *et al.* 2003) already exist, such observations for Greenland are very sparse. For West Greenland, the GPS site at Kellyville is the only source of information existing so far (Wahr *et al.* 2001a). Furthermore, in Fennoscandia, the ice load history ended some 8000 yr ago. In that region, all mass changes, which are now detected by satellites have to be attributed mainly to the ongoing post-glacial adjustment, besides

non-secular effects coming from oceanographic, atmospheric and hydrological contributions. In contrast to that, the ice load history in Greenland has to be extended to the present time. Therefore, the gravity signal caused by the viscoelastic reaction of the solid earth will be superimposed by the gravity effect of the recent mass balance of the Greenland ice sheet.

We will show that GPS observations in the ice-free area of West Greenland provide valuable information for the separation of these two main contributions of recent mass changes in that region. In addition, we will discuss the implications of the GPS observations concerning the present knowledge on sea-level changes, viscoelastic earth models as well as models and observations on past and present ice mass changes in West Greenland.

2 GEODETIC CONCEPT

In order to study the vertical crustal deformation pattern, a geodetic network has been established in the ice-free area of West Greenland (Fig. 1). This network was designed to utilize the GPS technique in an optimum way (Dietrich *et al.* 1998). In contrast to permanent observations, a campaign-style observation schedule was adopted. The network consists of 10 sites (Fig. 2, Table 1) and has a north–south extension of about 800 km. Two north–south profiles

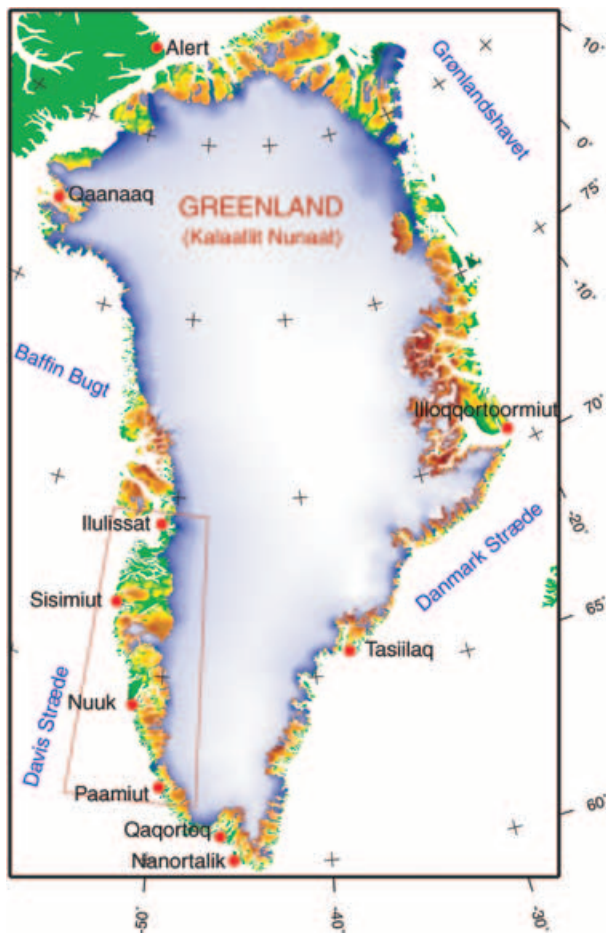


Figure 1. Overview of Greenland and the location of the area of investigation (marked by red box). Greenland covers an area of about $2.2 \times 10^6 \text{ km}^2$. The Greenland ice sheet covers an area of about $1.7 \times 10^6 \text{ km}^2$. Its volume amounts to about $2.9 \times 10^6 \text{ km}^3$ and its maximum thickness to 3200 m. The mean annual snow accumulation of about 600 km^3 (ice equivalent) is half-balanced by a loss through calving icebergs (Bennike *et al.* 2004). It is the only ice sheet that continues to exist in the northern hemisphere after the end of the last ice age. However, the retreat of the ice sheet after the last glacial maximum left an ice-free coastal zone which extends in West Greenland for up to 150 km (at 67°N). This is the region where our GPS network was set up (red box, cf. Fig. 2).

were set up: one profile along the ice edge and another one along the coast. This design also provides the possibility to form baselines in east–west direction, which enables the observation of the relative uplift between the coast and the ice edge.

Since (point) heights and height changes as observed by GPS are related to a global reference frame, the result is always directly affected by the realization and stability of this frame, especially by possible variations of the coordinate origin with respect to the earth's crust. For height differences within the network effects of the instability of the global reference frame are cancelled out to a great extent. Therefore, the regional pattern of relative uplift can be obtained with higher accuracy and reliability.

To realize this general approach, the following strategy was applied:

(i) The site Kangerlussuaq was chosen as the central site of the network and was observed during the entire time of each campaign. Only this station was linked to the global terrestrial reference frame.

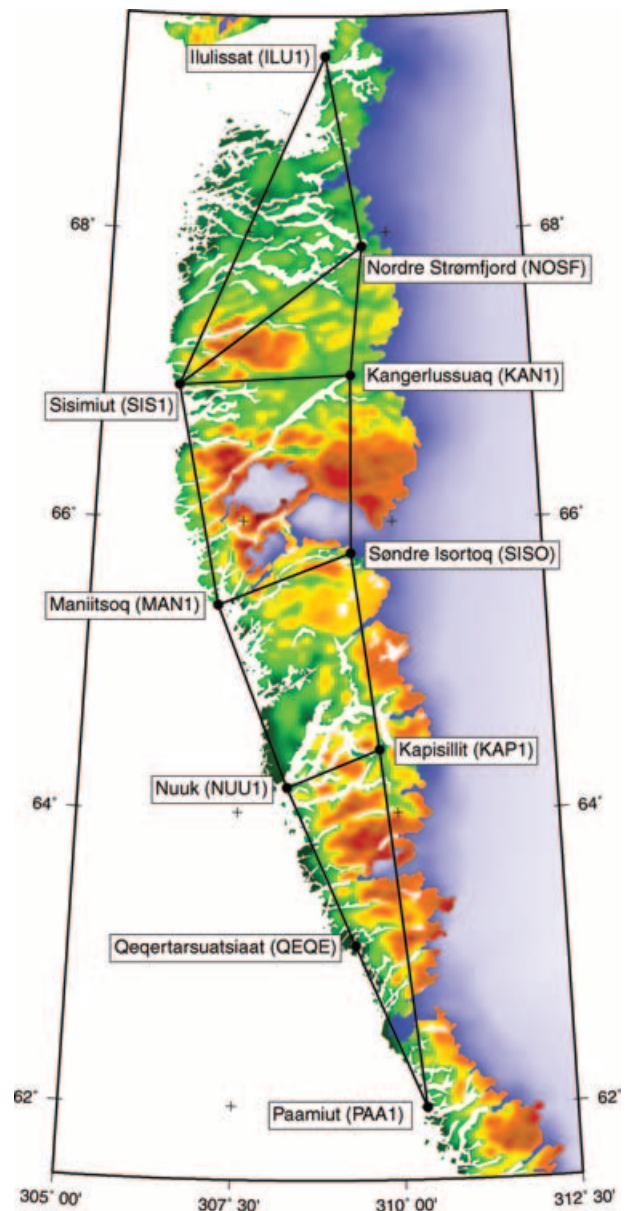


Figure 2. Overview of the geodetic network in West Greenland (See Fig. 1 for location of area of investigation.)

All other network sites were treated with respect to the central site Kangerlussuaq in order to get height differences and their temporal changes.

(ii) In addition to Kangerlussuaq, the sites Ilulissat, Kapisillit and Paamiut were occupied for approximately 20 days during each campaign to form the backbone of the network. Furthermore, two receivers were moved from south to north to carry out simultaneous observations at two further locations for at least 5 to 6 days each.

(iii) Within the West Greenland network, only one GPS receiver type was used (Trimble 4000). The site markers were monumented in bedrock to fix the antenna positions also during re-occupations by forced centring. For a specific site always the same individual antenna was used.

(iv) To keep possible seasonal effects on the results small, the campaigns were always performed at the same time of the year (August to early September).

Table 1. Observation sites of the West Greenland GPS network.

Station name	ID	Latitude		Longitude		Height [m]
		[deg min]		[deg min]		
Kangerlussuaq	KAN1	67	0	−50	41	61
Ilulissat	ILU1	69	13	−51	5	57
Norde Strømfjord	NOSF	67	53	−50	26	224
Sisimiut	SIS1	66	56	−53	40	85
Søndre Isortoq	SISO	65	47	−50	41	358
Maniitsoq	MAN1	65	24	−52	53	67
Nuuk	NUU1	64	10	−51	43	66
Kapisillit	KAP1	64	25	−50	16	116
Qeqertarsuaq	QEQE	63	5	−50	40	50
Paamiut	PAA1	61	59	−49	40	75

The first observation campaign was carried out in 1995. A complete re-observation took place in 2002. Between 1995 and 2002 smaller parts of the network, especially the baseline Kangerlussuaq–Sisimiut, were observed several times in order to get a better insight into the accuracy and significance of the obtained results. An overview of all observation campaigns is given in Table 2.

3 DATA ANALYSIS AND RESULTS

3.1 Data analysis: software, standards, models and parameterization

For the analysis of the GPS observations with the Bernese Software v5.0 (Hugentobler *et al.* 2004) internationally adopted standards were applied (McCarthy & Petit 2003). Aspects of the data processing, which are of special relevance for the determination of height changes from GPS observations, are described in the following.

In order to get homogeneous results for station coordinates, the utilization of homogeneous time series of GPS satellite orbits and earth orientation parameters is essential. The generally available time-series of the International GNSS Service (IGS) do not meet this requirement completely. During the period under consideration (1995–2002) different improvements were introduced into the routine processing at the IGS analysis centres. Furthermore, these IGS products refer to different reference system realizations (e.g. ITRF93 for the 1995 campaign or IGS00 system for the 2002 campaign). Therefore, the introduction of these IGS time series would cause inhomogeneities in the results, especially in the changes of the station coordinates with time. To overcome this problem, homogeneous time series of orbits and earth rotation parameters obtained by an ongoing reprocessing of the global GPS network (Rothacher *et al.* 2004) were introduced into the analysis.

All relevant geodynamic reductions were applied in order to enable a careful determination of heights and height changes. Especially, the effects caused by solid earth tides and ocean tidal loading have to be mentioned in this context. The ocean tidal loading was considered using the GOT00 model (Bos & Scherneck 2004). In midlatitudes, the displacement of the earth's crust due to atmospheric loading can reach peak-to-peak values of 10–20 mm (Rabbel & Zschau 1985). However, this effect was not introduced as a reduction into the analysis, but will be discussed in the following sections.

The effect of the signal path delay caused by the troposphere has to be taken into account very carefully. The tropospheric delay of the observations at different elevation angles is mapped to the zenith using Niell's mapping function (Niell 1996). In the parameter estimation, the station height and the tropospheric zenith path delay

Table 2. Number of observation days with at least 12 hr observation time.

Stat. ID	Year and day of year (DoY)				
	1995 220–246	1996 241–250	1997 246–254	2000 220–244	2002 211–244
KAN1	27	9	9	25	34
ILU1	21	–	–	3	22
NOSF	4	–	–	4	9
SIS1	9	6	6	9	9
SISO	7	–	–	5	7
MAN1	6	–	–	5	6
NUU1	6	–	–	–	7
KAP1	18	–	–	–	19
QEQE	8	–	–	–	7
PAA1	19	–	–	–	23

are correlated. In order to separate station height and tropospheric zenith path delay, observations at large zenith distances z are very important but were weighted using the weighting function $w(z) = \cos^2(z)$ (Rothacher & Beutler 1998). Therefore, the elevation cut-off angle used in the analyses was set to 10° . For each station the tropospheric zenith path delay was estimated for a time interval of 2 hr introducing the condition that the tropospheric delay changes only linear with time for each interval and that there are no jumps at the interval limits.

Antenna phase centre variations were taken into consideration using consistent, absolute models of both receiver and satellite antenna phase centres (Schmid & Rothacher 2003).

The processing of the GPS data using the Bernese Software comprises different steps. After an outlier detection procedure, the ambiguities were fixed to their integer values. For this purpose, different strategies were used depending on the baseline length. All parameters except station coordinates and troposphere parameters were pre-eliminated. The daily normal equation systems were combined and a campaign solution was computed. Finally, the normal equation systems of each campaign were combined again and three additional parameters per station were added to count for the change of the station coordinates with time. The solution of this normal equation system yielded a set of station positions for a specific epoch and a set of velocities.

3.2 Determination of the central site Kangerlussuaq in the global reference frame

According to the geodetic concept described in the previous section, in a first step coordinates and velocities of the central site Kangerlussuaq have to be determined within the global reference frame. For this purpose, the station was connected to surrounding IGS stations outside Greenland (Table 3, Fig. 3). The IGS realization IGB00 (Ray *et al.* 2004; IGB00 2004) was chosen as the terrestrial reference frame, which is a highly consistent solution based on about 100 well-established international GPS satellite tracking stations. The datum of this frame is identical to that of the International Terrestrial Reference Frame 2000 (ITRF2000) (Altamimi *et al.* 2002; Boucher *et al.* 2004), that is, the datum parameters (translation and rotation) are zero. Since the frame IGB00 was also introduced as a basis for the reprocessing of the global GPS network mentioned above the time-series of satellite orbits and earth rotation parameters are consistent with the station coordinates and velocities.

For each campaign daily coordinate solutions for Kangerlussuaq were obtained. The daily repeatability for the height component varies between 4.4 and 8.0 mm (Table 4). To calculate a formal error

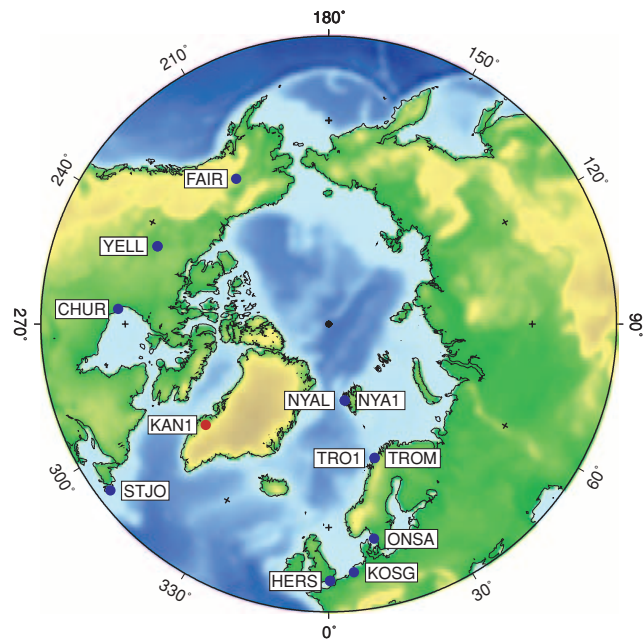


Figure 3. IGS stations used for the connection of the central site Kangerlussuaq (KAN1) to the global reference frame.

measure for the mean station height of each campaign, the number of observation days had to be taken into account. The values range between 0.8 and 1.9 mm (Table 4). This approach is based on the assumption that the time-series of GPS coordinates are uncorrelated (white noise model), which yields too optimistic results. In order to count for the correlation a power noise model can be used, which introduces a scaling of the error measure by a factor of 2. . . 5 (Zhang *et al.* 1997; Mao *et al.* 1999; Williams 2003; Williams *et al.* 2004). Thus, a more realistic error measure, applying a factor of 5, results in a range between 4.6 and 9.5 mm for the height component of one campaign solution.

Based on the campaign solutions the vertical rate for Kangerlussuaq was estimated to be $(-3.1 \pm 0.5) \text{ mm yr}^{-1}$, applying a linear regression (Fig. 4). The deviation of the individual campaign solutions from the linear trend opens another opportunity to estimate the height accuracy. The resulting rms value yields $\pm 3.1 \text{ mm}$ for one campaign solution, which proves the error estimation based on the daily repeatabilities.

However, some aspects have not been discussed so far. Long-term variations of station heights cannot be completely captured by campaign solutions. One contribution originates from an annual variation, which is clearly shown also for Greenland (Wahr *et al.* 2001a). Due to our observation concept the campaigns were carried out always at the same time of the year and, therefore, annual effects were cancelled out to a great extent. Another contribution originates from atmospheric loading, which was not introduced into the data reduction. Nevertheless, in order to estimate its magnitude, the products of the GGFC Special Bureau for Loading were used (van Dam *et al.* 2002). Within the observation campaigns, the vertical station displacement caused by atmospheric loading reaches a maximum peak-to-peak value of 12 mm at Kangerlussuaq. The mean values for each individual campaign vary between -2.8 and -1.4 mm (Table 5). Therefore, this effect on the vertical rate can be neglected. Nevertheless, considering the complete error budget for the vertical rate of Kangerlussuaq in the IGB00, we come up with an accuracy measure of $\pm 1.0 \text{ mm yr}^{-1}$, which is not a direct result

Table 3. GPS observing sites of the IGS used for the connection of the central site Kangerlussuaq (KAN1) to the global reference frame IGB00.

	1995	1996	1997	2000	2002
CHUR 40128M002		x	x	x	x
FAIR 40408M001	x	x	x	x	x
HERS 13212M007	x	x	x	x	x
KOSG 13504M003	x	x	x	x	x
NYAL 10317M001	x	x		x	x
NYA1 10317M003				x	x
ONSA 10402M004	x	x	x	x	x
STJO 40101M001	x	x	x	x	x
TROM 10302M003	x	x		x	x
TRO1 10302M006				x	x
YELL 40127M003	x	x	x	x	x

Table 4. Formal errors (in mm) of the station height at Kangerlussuaq for the five observation campaigns from 1995 to 2002.

	1995	1996	1997	2000	2002
Daily repeatability	5.4	5.8	4.6	8.0	4.4
Observation days	27	9	9	25	34
Formal height error	1.0	1.9	1.5	1.6	0.8

of the computations but is justified by the additional considerations outlined above.

The long-term stability of the underlying global reference frame is another important aspect which has to be considered in this context, especially regarding the realization of the origin (geocentre) of the frame with respect to the earth's crust (represented by the network stations). For the frame IGB00 that was applied in our analysis Ray *et al.* (2004) estimated an accuracy of $\pm 0.5 \text{ mm}$ and $\pm 1.0 \text{ mm}$ for the realization of the origin (translation), for the equatorial and axial components, respectively. The instability with time (rates for the equatorial components and the axial component, respectively) are estimated to be $\pm 0.2 \text{ mm yr}^{-1}$ and $\pm 0.35 \text{ mm yr}^{-1}$. Since our network is located in high latitudes we take the accuracy measure of the axial component and its long-term instability with $\pm 0.35 \text{ mm yr}^{-1}$.

Combining the error measure of $\pm 1.0 \text{ mm yr}^{-1}$ for the vertical rate at Kangerlussuaq and the accuracy of the long-term instability of the global reference frame of $\pm 0.35 \text{ mm yr}^{-1}$ we finally get an error measure of $\pm 1.1 \text{ mm yr}^{-1}$.

The IGS station Kellyville (KELY) was not introduced as a reference station for the connection of our network to the global reference frame and can now be used for an independent comparison of the results. It was set up (van Dam *et al.* 2000) in the same year when our first campaign took place (1995) and is situated at a distance of only 11.6 km from our central site Kangerlussuaq (KAN1). Due to this short distance between the two stations an identical vertical motion can be expected. In order to check this assumption the height difference between Kellyville and Kangerlussuaq was determined for each campaign (Fig. 5). Within the error measures the height difference is stable, except the value for 2002. This offset resulted from an antenna change at Kellyville in September 2001, which was also noticed by Nikolaidis (2002). Therefore, already published values of the vertical rate of Kellyville (Wahr *et al.* 2001a; Altamimi *et al.*

Table 5. Vertical displacement (in mm) due to air pressure loading: campaign mean for Kangerlussuaq (source: van Dam *et al.* 2002).

1995	1996	1997	2000	2002
-1.4	-1.7	-2.8	-2.8	-2.4

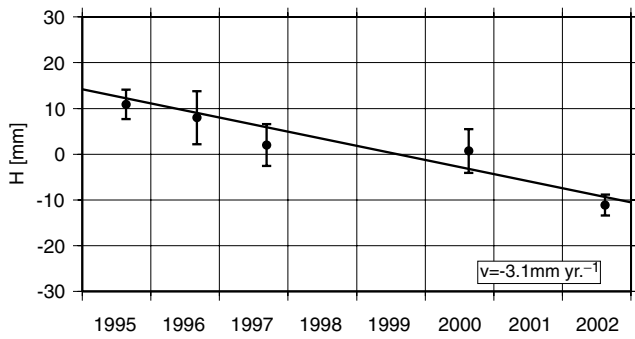


Figure 4. Campaign solutions for the station height and the inferred vertical velocity for Kangerlussuaq with respect to the reference frame IGB00 (mean height subtracted). Here and in the following figures error bars are computed from the formal mean height errors considering a power noise model (*cf.* text).

Table 6. Vertical velocities for Kellyville obtained by different data analyses.

Vertical velocity [mm yr ⁻¹]	rms [mm yr ⁻¹]	Reference
-5.8	±1.0	Wahr <i>et al.</i> (2001a)
-0.9	±1.1	Altamimi <i>et al.</i> (2002)
-2.0	±0.9	Nikolaidis (2002)
-3.1	±1.1	This investigation

2002; Nikolaidis 2002) can be compared to the vertical rate obtained for Kangerlussuaq. We think that the scatter of the solutions existing so far (Table 6) mainly reflects the uncertainty in the long-term stability of the different realizations of the global reference frame used in the different analyses as discussed above.

3.3 Estimation of relative vertical rates within the network

In the second step the coordinates and velocities of the central site Kangerlussuaq were fixed to the values obtained in the previous section. All other network stations were now determined with respect to Kangerlussuaq, that is, a baseline analysis was performed. As a typical example for one campaign solution, the 2002 results for the baseline from Kangerlussuaq (KAN1) to Paamiut (PAA1) (561 km) are shown in Fig. 6. Applying the same approach as in the previous section, we got a daily repeatability for the height difference of 3.6 mm. Considering the number of observation days and a scaling factor of 5 (according to the power noise model) the resulting error measure yields 3.9 mm. Furthermore, a satisfying decorrelation between daily height variations and relative tropospheric delay changes is visible. The differential atmospheric loading effect, which was computed using the data provided by the GGFC Bureau for Loading (van Dam *et al.* 2002), is in the order of 1. . . 2 mm and can therefore be neglected.

A more rigorous error evaluation could be performed for the baseline from Sisimiut (SIS1) to Kangerlussuaq (KAN1) (Fig. 7). This baseline was observed during five field campaigns between 1995 and 2002. We introduced the height differences of these five campaigns into a linear regression adjustment. The resulting rms value for the height difference of one campaign yields ±5.0 mm. This result is in accordance with the error estimate for the baseline KAN1 → PAA1 performed above, considering the lower number of observation days in the case of the baseline SIS1 → KAN1 (*cf.* Table 2). The rms value for the relative vertical rate resulting from

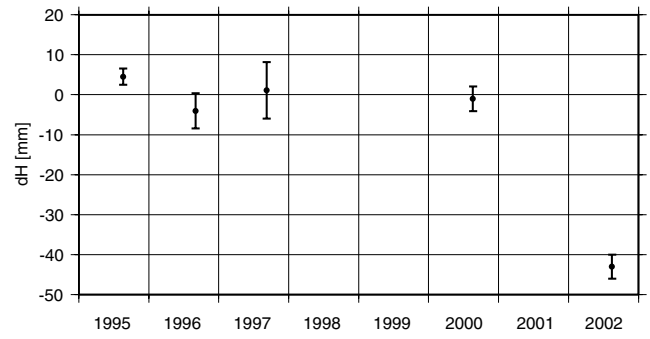


Figure 5. Height difference between Kellyville and Kangerlussuaq (mean of the campaign solutions 1995 to 2000 subtracted). The jump between 2000 and 2002 can be explained by changes in the antenna setup at Kellyville in 2001 September.

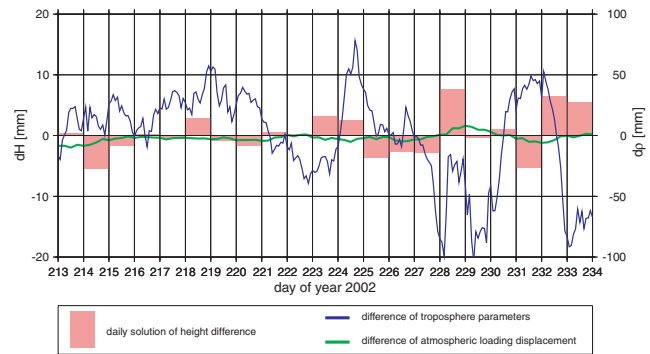


Figure 6. Daily solutions for the height difference dH of the baseline KAN1 → PAAM (561 km), (red bars, mean value subtracted). In addition, the estimated tropospheric zenith path delay $d\rho$ (blue line) and the differential vertical displacement due to atmospheric loading (green line) are shown.

this regression yields ±1.0 mm yr⁻¹. This value of ±1.0 mm yr⁻¹ could be taken as a sound error estimate for the relative vertical rates of the entire network, since the number of observation days for the baseline SIS1 → KAN1 is at the lower limit of observation days of all network sites.

Dealing with the baseline approach and thus with relative height changes within the network, effects coming from remaining uncertainties of the long-term stability of the global reference frame (as discussed in the previous section) are reduced to a large extent. Therefore, further error components have not to be considered in the error budget.

3.4 Final results and their accuracies

The final results were obtained by a combination of all campaign solutions at the level of normal equations. For every site of the West Greenland network, coordinates and velocities were estimated relative to Kangerlussuaq. In this way a rigorous adjustment could be performed. The central station Kangerlussuaq was linked to the global reference frame as described in Section 3.2. The resulting vertical rates obtained for all sites in West Greenland are summarized in Table 7 and—regarding the relative rates—in Table 8. Following the discussion in the previous sections, we came up with a realistic accuracy measure of ±1.5 mm yr⁻¹ for all other network sites, combining the accuracy of ±1.1 mm yr⁻¹ for Kangerlussuaq and of ±1.0 mm yr⁻¹ for the relative rates within the West Greenland network. The vertical rates as shown in Table 7 provide the input for

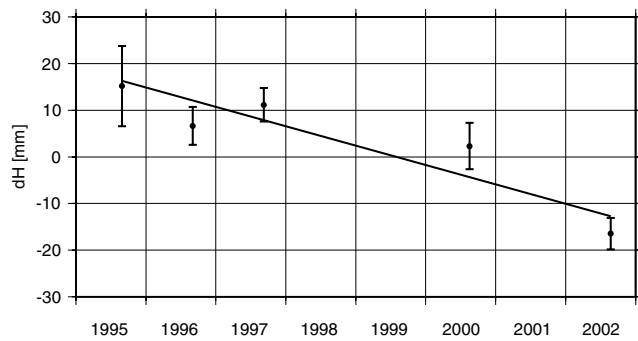


Figure 7. Campaign solutions for the height difference of the baseline from Sisimiut (SIS1) to Kangerlussuaq (KAN1). The inferred height difference change yields -4.1 mm yr^{-1} (cf. Table 8).

a map of the spatial pattern of the recent crustal deformation in West Greenland (Fig. 8), which is a vivid basis for further interpretation.

4 DISCUSSION

4.1 Implications for models of ice load history and of the viscoelastic earth

It is well known, that the Greenland ice sheet was larger at the last glacial maximum (LGM) than at present. Since the LGM the total ice volume has decreased by 15...20 per cent (Le Meur & Huybrechts 1998). Simultaneously to the melting a remarkable retreat of the ice margin occurred. In West Greenland, the LGM ice margin could be located up to 150 km west of its present position at the coastal shelf (Weidick 1993). The retreating ice margin left a wealth of geomorphological traces and features, which were used for a reconstruction of this retreat (van Tatenhove *et al.* 1995, 1996b). The dated moraines indicate that the retreat started about 12 000 yr BP. In the Kangerlussuaq area at about 67°N the location of the present margin was reached already 7000 yr BP (van Tatenhove *et al.* 1996b). Model calculations show, that this retreat continued in this area until the ice margin reached a position of about 60 km east of the present margin (see van Tatenhove *et al.* 1996a). This corresponds to a Holocene minimum of the ice volume at about 4000 yr BP and a re-advance, especially in West Greenland, which began at that time. A retreat of an ice mass is easy to trace in the field due to the existing geomorphological features in contrast to a re-advance in former times, since the re-advancing ice overruns any older evidence. Therefore, one has to utilize indirect indications like sea-level curves and vertical crustal motions. Also, it is difficult to validate the impact of climate change on ice margin changes in West Greenland within the last 2000 yr. There is some evidence on smaller variations with phases of advance and retreat (Weidick 1996a). In general, model runs demonstrate that the western margin of the Greenland ice sheet is rather sensitive with respect to changes of environmental parameters (Huybrechts *et al.* 2002). For the last century, Weidick (1991) documented regions of ice advance and of ice recession at the ice margin of West Greenland. Comparing the state of 1950 with that of 1985, there are even areas where the local mass balance changed its sign (Weidick 1991).

Based on the ICE-3G ice load history (Tushingham & Peltier 1991) earlier model predictions of vertical crustal motions showed an uplift gradient positive from the coast in direction to the ice margin in the order of 1...3 mm/100 km (Mitrovica *et al.* 1994). Modified model calculations, which include the Holocene re-advance

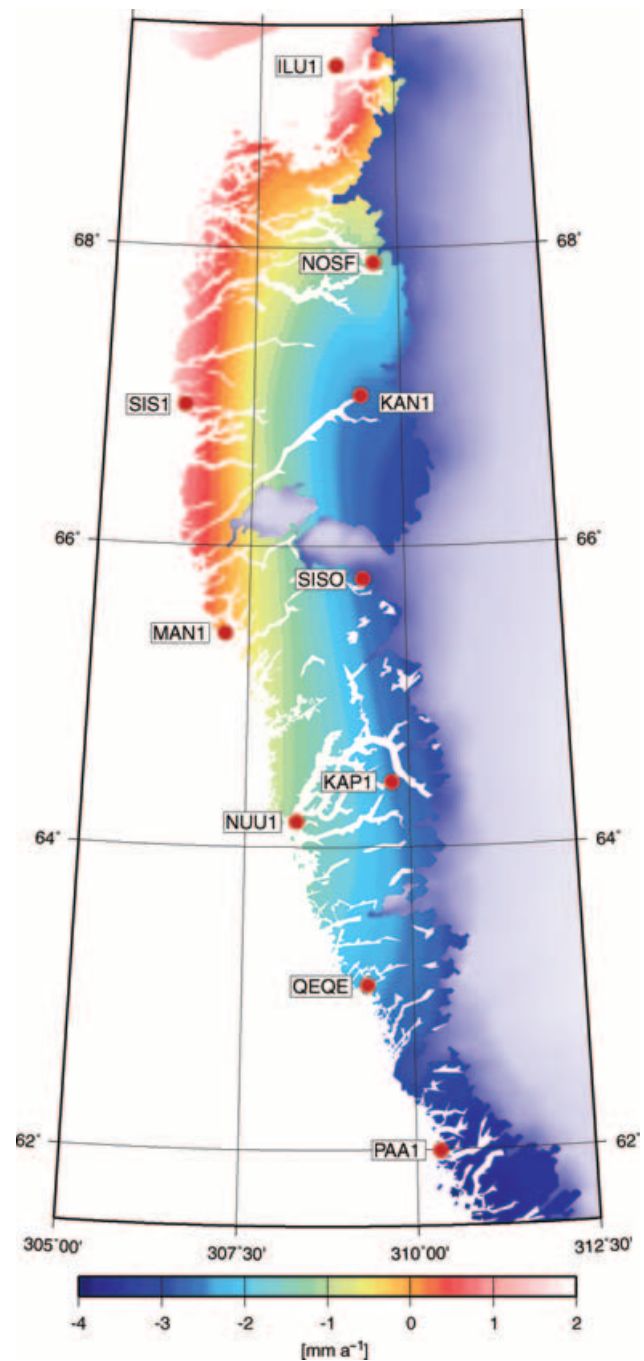


Figure 8. Map of vertical crustal deformations in West Greenland as obtained from repeated GPS observations.

(Huybrechts *et al.* 2002) as mentioned in Section 2, yielded negative uplift (i.e. subsidence) areas close to the West Greenland ice margin (Wahr *et al.* 2001a; Tarasov & Peltier 2002). Until now, the permanent GPS site Kellyville has presented the only geodetic option for a verification of these different model predictions.

Our results can now be used to compare the different model predictions performed by Tarasov & Peltier (2002) and Wahr *et al.* (2001b). Since we are faced with an inverse problem, which has not a unique solution, an improvement of both the ice load history model and the rheological model of the earth would result in a variety of different sets of the relevant parameters. As it was pointed out, for

Table 7. Estimated vertical velocities v_H for the West Greenland GPS sites (IGb00 reference frame).

Station name	ID	Latitude		Longitude		v_H [mm yr ⁻¹]
		[deg min]		[deg min]		
Kangerlussuaq	KAN1	67	0	-50	41	-3.1
Ilulissat	ILU1	69	13	-51	5	1.6
Nordre Strømfjord	NOSF	67	53	-50	26	-1.2
Sisimiut	SIS1	66	56	-53	40	1.0
Søndre Isortoq	SISO	65	47	-50	41	-2.5
Maniitsoq	MAN1	65	24	-52	53	-0.2
Nuuk	NUU1	64	10	-51	43	-1.0
Kapisillit	KAP1	64	25	-50	16	-2.2
Qeqertarsuaatsiaat	QEQE	63	5	-50	40	-2.8
Paamiut	PAA1	61	59	-49	40	-3.4

example, by Wahr *et al.* (2001b), especially changes in either the viscosity, the lithospheric thickness or the time evolution of the ice load may lead to similar predictions of the present-day vertical deformation. Nevertheless, the spatial deformation pattern resulting from our analysis (Fig. 8) confirms the general findings stating a negative uplift along the ice margin caused by a late Holocene re-advance of the ice sheet. One interesting new aspect is that, south of the central site Kangerlussuaq, the vertical motions along the ice margin up to the southernmost site of our network remain almost constant. This means, that especially in the southern region around Paamiut, the re-advance of the ice sheet was of a larger magnitude than assumed in the models so far, or other re-advance events occurred later. The large relative uplift of 4.7 mm yr⁻¹ of the Disko Bay region (Ilulissat) with respect to Kangerlussuaq is another interesting result of our investigation, which cannot completely be explained by the late Holocene re-advance. This feature will be discussed in more detail in Section 4.3. The spatial uplift pattern, especially concerning the gradients between the coast and the ice margin, would show a best agreement with model predictions using a lithospheric thickness of 80 to 90 km and a viscosity of the upper mantle of $6 \cdot 10^{20}$ Pa s (Wahr *et al.* 2001b), which are also close to the parameters obtained by Tarasov & Peltier (2002).

4.2 Consequences for sea-level trends in West Greenland

In order to interpret the obtained vertical motions as shown in Fig. 8 with respect to present-day sea-level changes in West Greenland one has to keep in mind that relative sea-level changes are a combined effect of bedrock displacement, ocean volume change and geoid adjustment. The bedrock displacement is observed by GPS. To estimate the influence of the ocean volume change (eustatic effect) one has to utilize additional information. In general, the resulting geoid effect would be considerably smaller than the eustatic effect (Peltier 1998; Ivins *et al.* 2001; Le Meur & Huybrechts 2001; Fleming *et al.* 2004). Therefore, only the dominating eustatic effect will be considered in the following. For the 20th century the eustatic effect was determined from global tide gauge data to be 1.8 ± 0.5 mm a⁻¹ (Church *et al.* 2001, p. 662). This value is a global average for one century. Short-term and regional variations of the sea level also occur but are not discussed here. In order to estimate the relative sea-level change at the coast of West Greenland for the last 100 yr, the vertical motion determined by GPS has to be subtracted from the eustatic sea-level rate. To give an error prediction for this relative sea-level change, the error measures of the eustatic sea-level change and the GPS-derived vertical motions have to be considered jointly, which yields a rms of ± 1.6 mm yr⁻¹. Now the pattern of

Table 8. Estimated relative vertical velocities dv_H for baselines in the West Greenland GPS network.

Baseline	Baseline length [km]	dv_H [mm yr ⁻¹]
SIS1 → KAN1	131	-4.1
MAN1 → SISO	109	-2.3
NUU1 → KAP1	77	-1.2
KAN1 → ILU1	248	+4.7
KAN1 → NOSF	100	+1.9
SISO → KAN1	136	-0.6
KAP1 → KAN1	288	-0.9
QEQE → KAP1	151	+0.6
PAA1 → KAP1	274	+1.2

the relative sea-level change in West Greenland can be discussed in detail.

At the outer coast in the northern part of our area of investigation (from Sisimiut up to Ilulissat) the present-day sea-level change is almost zero within the error limits mentioned above. Going from Maniitsoq towards the southern coastal parts and going from the coast eastwards into the fjords towards the inland ice margin, the relative sea level shows an increasing tendency to rise, with rates of 2.8 mm yr⁻¹ in Nuuk, 5.2 mm yr⁻¹ in Paamiut and 2.8 . . . 4.9 mm yr⁻¹ in the innermost parts of Nordre Strømfjord, Søndre Strømfjord, Søndre Isortoq and Nuuk Fjord.

In the context of long-term trends the obtained results fit to most of the observations and existing scenarios. For the coastal area of West Greenland hundreds of shell samples were dated and used in order to construct emergency curves for different regions (Kelly 1973, 1979; TenBrink 1974; Donner & Jungner 1975). Weidick (1996a) compiled a map of the upper level of marine deposits (Fig. 9). For the coastal area between 67°N and 68°N this map shows a maximum of more than 120 m above the present sea level and a slope towards the inland ice. The reconstruction revealed that the historic sea level reached the present sea level at about 3000 . . . 4000 yr BP (Weidick 1996b). This is the consequence of the early–middle Holocene deglaciation of the area and the late Holocene re-advance of the ice sheet about 4000 yr BP as described in the previous section.

Consequently, it is rather difficult to reconstruct a late Holocene sea level, which is below the present one. To pursue this task, archaeological investigations provided additional information. Greenland has been inhabited for about 4500 yr by different Inuit cultures. For West Greenland, the Saqqaq period (about 4400–2800 yr BP), the Dorset period (about 2600–1800 yr BP) and the Thule period (after 900 yr BP) are proven. Furthermore, the Norsemen inhabited two main settlements in West and South Greenland between 1000 and 600 yr BP. Both the Inuit and the Norsemen very often settled close to the sea. Between settlements of different ages archaeologists documented considerable elevation differences with respect to the present sea level. For instance, in the Sisimiut district all documented coastal Saqqaq sites are situated at a height of 12 m and more above present sea level, whereas the Dorset sites range between 4 . . . 8 m (Kramer 1996). Kramer (1996) even argues that it is likely that some Dorset localities are now submerged. For the Nuuk Fjord area the submerged Norseman church at Sandnes is a well-known example (Weidick 1976). Clear evidence for submerged archaeological sites is reported for the southern Disko Bay, which will be discussed in more detail in the following section. Weidick (1996b) tried to summarize all glaciological, archaeological and historical evidence in order to reconstruct sea-level changes in West Greenland. He stated a sea-level rise in the order of several metres for the last 1000 yr, at

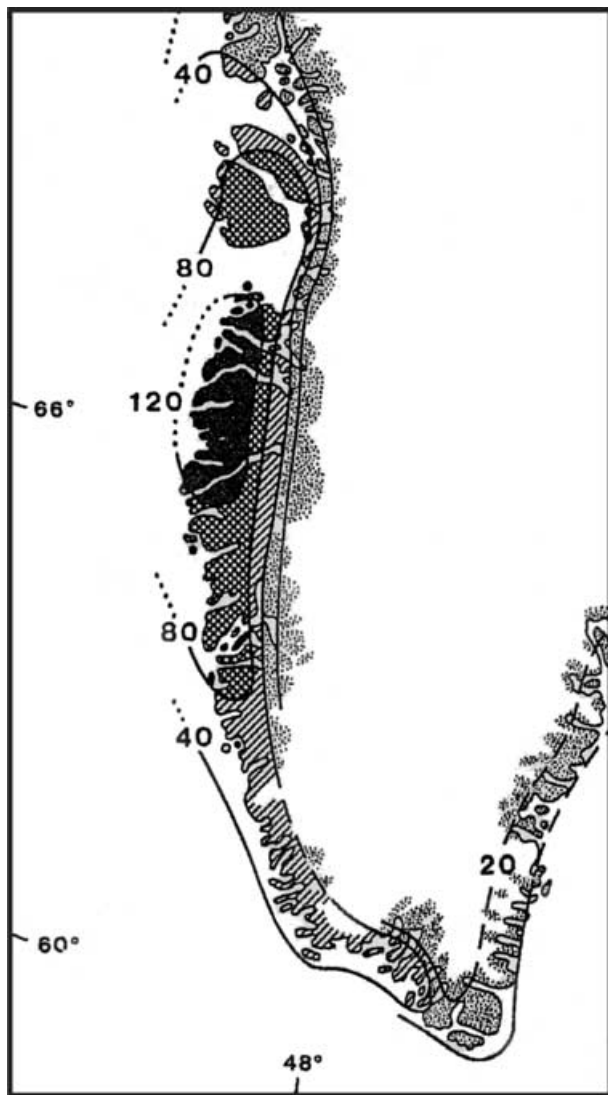


Figure 9. Upper level of marine deposits in West Greenland (from Weidick 1996a with kind permission of the author and of the Zeitschrift für Gletscherkunde und Glazialgeologie).

least for most parts of the coast, which is not in contradiction with our results.

4.3 The Disko Bay region and the imprint of the Jakobshavn Isbræ

The large vertical velocity difference of 4.7 mm yr^{-1} between Kangerlussuaq and Ilulissat is an interesting result of our investigations, yielding an uplift rate for Ilulissat of $+1.6 \text{ mm yr}^{-1}$. As discussed in the previous section the estimated relative sea-level change in Ilulissat would be almost zero (within the error band of $\pm 1.6 \text{ mm yr}^{-1}$). Recalling glaciological, geomorphological and archaeological facts, the early–middle Holocene retreat of the ice margin is evident also in this region (Weidick *et al.* 1990; Rasch 2000). The ice margin reached the position of the present ice margin about 6000 yr BP and continued to retreat further east for about 20 km about 4000 BP (Weidick *et al.* 1990). The later re-advance of the ice sheet in West Greenland and also in the Disko Bay region is the main reason that the historic sea level about 3000–4000 yr BP was at the height of the present-day sea level, and that the lowest level of the

sea is assumed for 1000–2000 yr BP (Rasch 2000). Archaeological investigations of submerged Dorset dwelling sites in the southern Disko Bay clearly indicate a sea level being 2.0–2.5 m below the present one (Rasch & Jensen 1997). Furthermore, there is archaeological and geomorphological evidence that a further transgression started about 1000 yr BP (Rasch & Jensen 1997; Rasch 2000). This sea-level rise continued almost to the present time, since there are also dwelling sites of the Thule culture related to the 17th century, which are flooded now at high tide (Rasch & Jensen 1997). The advance of the Jakobshavn Isbræ during the Little Ice Age (Weidick *et al.* 1990) should have increased the subsidence rate because of an increased surface load, which corresponds to a transgression for the last centuries as reported above.

How do these findings fit to the present-day vertical rate of Ilulissat as observed by GPS? We conclude that the retreat of the Jakobshavn Isbræ during the last 150 yr—considering the associated mass losses at the ice margin and within the drainage basin of the glacier—causes an additional uplift component, which presently superimposes the long-term trend in that area.

The retreat of the glacier front and the surrounding ice margin started about 150 yr ago (Weidick 1992). Although the retreat of the floating glacier tongue alone would not change the surface load there is clear evidence of a retreat of the ice margin next to the glacier by an amount of up to several kilometres (Weidick 1992). Recent glaciological investigations indicate that the surface height of the ice is presently decreasing as well. Although repeated laser scanner observations yield a thickening of the Jakobshavn Isbræ from 1991 to 1997 at elevations less than 1100 m (Krabill *et al.* 2000), they show surface heights decreasing in the order of -10 cm yr^{-1} at the drainage basin of the Jakobshavn Isbræ between 50°W and 42°W (Krabill *et al.* 2000). Further mass balance studies reveal also a thinning of $(6.2 \pm 2.7) \text{ cm yr}^{-1}$ for the higher elevation part of the drainage basin (Thomas *et al.* 2000). Recently, the glacier flow velocity was investigated to be almost constant at 5700 m yr^{-1} from 1992 to 1997, but to be accelerated up to 12600 m yr^{-1} in 2003 (Joughin *et al.* 2004), which was found to sufficiently explaining observed elevation changes as dynamic thickening (in the early 1990s) and thinning (thereafter). For the time period after 1997 an increasing rate of thinning was observed also in the low elevation area of the Jakobshavn Isbræ with magnitudes of about 1 m yr^{-1} (Krabill *et al.* 2004). These are clear indications for an ongoing negative mass balance of the Jakobshavn Isbræ and its drainage basin which should also lead to an increase of the associated crustal uplift signal at Ilulissat.

5 CONCLUSIONS

Our results show that the concept of campaign-type GPS observations could successfully be applied to the determination of the vertical crustal deformations in West Greenland. The obtained vertical velocities can serve as an additional source of information to validate and improve both models on the glacial history of the Greenland ice sheet and models of the viscoelastic response of the earth. The results provide an alternative approach to investigate recent sea-level trends in Greenland and may, therefore, help to understand historical sea-level changes associated with archaeological investigations in West Greenland. Thus, there are several interdisciplinary aspects, which can be addressed in collaboration with neighbouring disciplines.

If a third re-observation of the network is carried out thus prolonging the time basis, a further improvement of the obtained accuracies will be possible. A global reference frame with improved

consistency and long-term stability can then be expected and would contribute to higher accuracies as well.

Already now the regional pattern of the vertical deformation can be used as additional information for the analysis of gravity field changes, utilizing satellite missions like GRACE, in order to separate the different sources of recent mass changes in Greenland.

ACKNOWLEDGMENTS

Many people supported the idea to investigate vertical crustal deformations in Greenland and provided valuable advice to realize the project. Special thanks go to: René Forsberg, Frede Madsen and Finn Bo Madsen at Kort- og Matrikelstyrelsen (KMS Copenhagen, Denmark); Anker Weidick at Danmarks og Grønlands Geologiske Undersøgelse (GEUS Copenhagen, Denmark, now retired); Henning Thing at the Danish Polar Center (Copenhagen, Denmark); Philippe Huybrechts at Alfred Wegener Institute for Polar and Marine Research (AWI Bremerhaven, Germany).

The Danish Polar Center (Copenhagen, Denmark) supported our work by granting permissions for the field work and by providing the facilities at the Kangerlussuaq International Science Support (KISS). The kind collaboration with Air Greenland (Nuuk, Greenland) that provided helicopter charters is gratefully acknowledged. We are especially thankful to many responsible people at the local authorities in West Greenland who provided their support. Furthermore, we would also like to acknowledge the warm reception by all people of Greenland, who helped us a lot to get into contact, to organize accommodation and means of transport and thus to realize our research work.

Last but not least we would like to thank all (former and present) colleagues and students of our institute who participated in the observation campaigns in West Greenland: Doreen Adler, Wieland Adler, Michael Bäßler, Lutz Eberlein, Martin Horwath, Wilfried Korth, Gunter Liebsch, Ulrike Oelsner, Swen Roemer, Waldemar Schneider, Heiko Sievers, Steven Sonntag, Susan Thoß, Anja Wendt, and Jens Wendt.

Maps were drawn using topographic data provided by Kort- og Matrikelstyrelsen (Ekholm 1996) and the mapping software GMT 3.4 (Wessel & Smith 1991). We thank two anonymous reviewers for their helpful comments.

The German Research Foundation (DFG) supported this long-term project by several research grants which is gratefully acknowledged.

REFERENCES

- Altamimi, Z., Sillard, P. & Boucher, C., 2002. ITRF2000: A new release of the International Terrestrial Reference Frame for earth science applications, *J. geophys. Res.*, **107**(B10), 2214, doi:10.1029/2001JB000561.
- Bennike, O., Mikkelsen, N., Pedersen, H.K. & Weidick, A., eds., 2004. *Ilulissat Icefjord—A World Heritage Site*, Danmarks og Grønlands Geologiske Undersøgelse (GEUS), Copenhagen.
- Bos, M.S. & Scherneck, H.G., 2004. Free ocean tide loading provider, <http://www.oso.chalmers.se/loading/>.
- Boucher, C., Altamimi, Z., Sillard, P. & Feissel-Vernier, M., 2004. The ITRF2000 IERS Technical Note No. 31, Verlag des Bundesamtes für Kartographie und Geodäsie, Frankfurt am Main.
- Church, J.A., Gregory, J.M., Huybrechts, P., Kuhn, M., Lambeck, K., Nhuan, M.T., Qin, D. & Woodworth, P.L., 2001. Changes in Sea Level, in *Climate Change 2001: The Scientific Basis*, chap. 11, pp. 639–693, eds Houghton, J.T., Ding, Y., Griggs, D.J., Noguer, M., van der Linden, P.J., Dai, X., Maskell, K. & Johnson, C.A., Cambridge University Press (Contribution of Working Group I to the Third Assessment Report of the Intergovernmental Panel on Climate Change), Cambridge, UK.
- Dietrich, R., Scheinert, M. & Korth, W., 1998. The verification of the solid Earth response on changing ice loads: a geodetic project in West Greenland, in *Dynamics of the Ice Age Earth: A Modern Perspective. GeoResearchForum*, Vols 3–4, pp. 509–522, ed. Wu, P., Trans Tech Publications Ltd., Uetikon-Zürich, Switzerland.
- Donner, J. & Jungner, H., 1975. Radiocarbon dating of shells from marine Holocene deposits in the Disko Bugt area, West Greenland, *Boreas*, **4**, 25–45.
- Ekholm, S., 1996. A full coverage, high resolution, topographic model of Greenland, computed from a variety of digital elevation data, *J. geophys. Res.*, **101**(B10), 21 961–21 972.
- Ekman, M., 1993. Postglacial rebound and sea level phenomena, with special reference to Fennoscandia and the Baltic Sea, in *Geodesy and Geophysics*, pp. 7–70, ed. Kakkuri, J., Publications of the Finnish Geodetic Institute, Helsinki, 115.
- Ekman, M. & Mäkinen, J., 1996. Recent postglacial rebound, gravity change and mantle flow in Fennoscandia, *Geophys. J. Int.*, **126**(1), 229–234.
- Fleming, K., Martinec, Z. & Hagedoorn, J., 2004. Geoid displacement about Greenland resulting from past and present-day mass changes in the Greenland ice sheet, *Geophys. Res. Lett.*, **31**, L06617, doi:10.1029/2004GL019469.
- Hugentobler, U., Dach, R. & Fridez, P., eds., 2004. *Bernese GPS Software, Version 5.0*, University of Bern, Draft.
- Huybrechts, P., Janssens, I., Poncin, C. & Fichet, T., 2002. The response of the Greenland ice sheet to climate changes in the 21st century by interactive coupling of an AOGCM with a thermomechanical ice-sheet model, *Annals of Glaciology*, **35**, 409–415.
- IGb00, 2004. igsb.jpl.nasa.gov/network/iframe.html.
- Ivins, E.R., Wu, X., Raymond, C.A., Yoder, C.F. & James, T.S., 2001. Temporal Geoid of a Rebounding Antarctica and Potential Measurement by the GRACE and GOCE Satellites, in *Gravity, Geoid and Geodynamics 2000, IAG Symposia*, Vol. 123, pp. 361–366, ed. Sideris, M., Springer Heidelberg, Berlin.
- Joughin, I., Abdalati, W. & Fahnestock, M., 2004. Large fluctuations in speed on Greenland's Jakobshavn Isbræ glacier, *Nature*, **432**, 608–610, doi:10.1038/nature03130.
- Kelly, M., 1973. Radiocarbon dated shell samples from Nordre Strømfjord, West Greenland, with comments on models of glacio-isostatic uplift, *Rapp. Grønlands geol. Unders.*, **59**.
- Kelly, M., 1979. Comments on the implications of new radiocarbon datings from the Holsteinsborg region, central West Greenland, *Rapp. Grønlands geol. Unders.*, **95**, 35–42.
- Krabill, W. et al., 2000. Greenland ice sheet: high-elevation balance and peripheral thinning, *Science*, **289**, 428–430.
- Krabill, W. et al., 2004. Greenland ice sheet: increased coastal thinning, *Geophys. Res. Lett.*, **31**(24), doi:10.1029/2004GL021533.
- Kramer, F.E., 1996. The Paleo-Eskimo cultures in Sisimiut District, West Greenland: aspects of chronology, in *The Paleo-Eskimo Cultures of Greenland*, pp. 39–63, Grønnow, B., Danish Polar Center, Copenhagen.
- Le Meur, E. & Huybrechts, P., 1998. Present-day uplift pattern over Greenland from a coupled ice-sheet/visco-elastic bedrock model, *Geophys. Res. Lett.*, **25**(21), 3951–3954.
- Le Meur, E. & Huybrechts, P., 2001. A model computation of the temporal changes of surface gravity and geoidal signal induced by the evolving Greenland ice sheet, *Geophys. J. Int.*, **145**, 835–849.
- Mäkinen, J., Koivula, H., Poutanen, M. & Saarinen, V., 2003. Vertical velocities in Finland from permanent GPS networks and from repeated precise levelling, *J. Geodyn.*, **35**, 443–456.
- Mao, A., Harrison, C.G.A. & Dixon, T.H., 1999. Noise in GPS coordinate time series, *J. geophys. Res.*, **104**(B2), 2797–2816, doi:10.1029/1998JB900033.
- McCarthy, D.D. & Petit, G., 2003. IERS Conventions 2003, IERS Technical Note No. 32 Verlag des Bundesamtes für Kartographie und Geodäsie, Frankfurt am Main.

- Mitrovica, J.X., Davis, J.L. & Shapiro, I.I., 1994. A spectral formalism for computing three-dimensional deformations due to surface loads 2. Present-day glacial isostatic adjustment, *J. geophys. Res.*, **99**(B4), 7075–7101.
- Niell, A.E., 1996. Global mapping functions for the atmosphere delay at radio wavelengths, *J. geophys. Res.*, **101**(B2), 3227–3246.
- Nikolaidis, R., 2002. Observation of geodetic and seismic deformation with the Global Positioning System, *PhD thesis*, University of California, San Diego.
- Peltier, W.R., 1998. Postglacial variations in the level of the sea: implications for climate dynamics and solid-earth physics, *Reviews of Geophysics*, **36**(4), 603–689.
- Rabbet, W. & Zschau, J., 1985. Static deformations and gravity changes at the earth's surface due to atmospheric loading, *J. Geophys.*, **56**, 81–99.
- Rasch, M., 2000. Holocene relative sea level changes in Disko Bugt, West Greenland, *Journal of Coastal Research*, **16**(2), 306–315.
- Rasch, M. & Jensen, J.F., 1997. Ancient Eskimo dwelling sites and Holocene relative sea-level changes in southern Disko Bugt, central West Greenland, *Polar Research*, **16**(2), 101–115.
- Ray, J., Dong, D. & Altamimi, Z., 2004. IGS reference frames: status and future improvements, *GPS Solutions*, **8**(4), 251–266, doi:10.1007/s10291-004-0110-x.
- Rothacher, M. & Beutler, G., 1998. The Role of GPS in the Study of Global Change, *Physics and Chemistry of the Earth*, **23**(9–10), 1029–1040.
- Rothacher, M., Steigenberger, P., Dietrich, R., Fritsche, M. & Rülke, A., 2004. Reprocessing of the Global GPS network—first results, poster presentation, IGS Workshop, Bern.
- Scherneck, H.G., Johansson, J.M., Koivula, H., van Dam, T. & Davis, J.L., 2003. Vertical crustal motion observed in the BIFROST project, *J. Geodyn.*, **35**, 425–441.
- Schmid, R. & Rothacher, M., 2003. Estimation of elevation-dependent satellite antenna phase center variations of GPS satellites, *Journal of Geodesy*, **77**, 440–446, doi: 10.1007/s00190-003-0339-0.
- Tarasov, L. & Peltier, W.R., 2002. Greenland glacial history and local geodynamic consequences, *Geophys. J. Int.*, **150**(1), 198–229.
- TenBrink, N., 1974. Glacio-isostasy: new data from West Greenland and new geophysical implications, *Geol. Society America Bull.*, **85**, 219–228.
- Thomas, R., Akins, T., Csatho, B., Fahnestock, M., Gogineni, P., Kim, C. & Sonntag, J., 2000. Mass balance of the Greenland ice sheet at high elevations, *Science*, **289**, 426–428.
- Tushingham, A.M. & Peltier, W., 1991. ICE-3G: A new global model of late Pleistocene deglaciation based upon geophysical predictions of post-glacial relative sea-level change, *J. geophys. Res.*, **96**, 4497–4523.
- van Dam, T., Wahr, J., Gross, S. & Francis, O., 2000. Using GPS and gravity to infer ice mass changes in Greenland, *EOS, Trans. Am. geophys. Un.*, **81**(37), 421, 426–427.
- van Dam, T., Plag, H.-P., Francis, O. & Gegout, P., 2002. GGFC Special Bureau for Loading: current status and plans, in *Proceedings of the IERS Workshop on Combination Research and Global Geophysical Fluids*, pp. 180–198, eds Richter, B., Schwegmann, W. & Dick, W.R., IERS Technical Note No. 30, Verlag des Bundesamtes für Kartographie und Geodäsie, Frankfurt am Main.
- van Tatenhove, F.G.M., van der Meer, J.J.M. & Huybrechts, P., 1995. Glacial-geological/geomorphological research in West Greenland used to test an ice-sheet model, *Quaternary Research*, **44**, 317–327.
- van Tatenhove, F.G.M., Fabre, A., Greve, R. & Huybrechts, P., 1996a. Modelled ice-sheet margins of three Greenland ice-sheet models compared with a geological record from ice-marginal deposits in central West Greenland, *Annales Glaciology*, **23**, 52–58.
- van Tatenhove, F.G.M., van der Meer, J.J.M. & Koster, E.A., 1996b. Implications for deglaciation chronology from New AMS age determinations in Central West Greenland, *Quaternary Research*, **45**, 245–253.
- Wahr, J., van Dam, T., Larson, K. & Francis, O., 2001a. Geodetic measurements in Greenland and their implications, *J. geophys. Res.*, **106**(B8), 16 567–16 581.
- Wahr, J., van Dam, T., Larson, K. & Francis, O., 2001b. GPS measurements of vertical crustal motion in Greenland, *J. geophys. Res.*, **106**(D24), 33 755–33 759.
- Weidick, A., 1976. Glaciation and the Quaternary, in *Geology of Greenland*, pp. 431–458, eds Escher, A. & Watt, S., Grønlands Geologiske Undersøgelse, Copenhagen.
- Weidick, A., 1991. Present-day expansion of the southern part of the Inland Ice, *Rapp. Grønlands geol. Unders.*, **152**, 73–79.
- Weidick, A., 1992. Jakobshavn Isbræ area during the climatic optimum, *Rapp. Grønlands geol. Unders.*, **155**, 67–72.
- Weidick, A., 1993. Neoglacial change of ice cover and the related response of the Earth's crust in West Greenland, *Rapp. Grønlands geol. Unders.*, **159**, 121–126.
- Weidick, A., 1996a. Late Holocene and historical changes of glacier cover and related relative sea level in Greenland, *Zeitschrift für Gletscherkunde und Glazialgeologie*, **32**, 217–224.
- Weidick, A., 1996b. Neoglacial changes of ice cover and sea level in Greenland—a classical enigma, in *The Paleo-Eskimo Cultures of Greenland*, pp. 257–270, eds Grønnow, B., Danish Polar Center, Copenhagen.
- Weidick, A., Oerter, H., Reeh, N., Thomsen, H.H. & Thorning, L., 1990. The recession of the Inland Ice margin during the Holocene climatic optimum in the Jakobshavn Isfjord area of West Greenland, *Palaeogeography, Palaeoclimatology, Palaeoecology*, **82**, 389–399.
- Wessel, P. & Smith, W.H.F., 1991. Free software helps map and display data, *EOS, Trans. Am. geophys. Un.*, **72**, 441.
- Williams, S.D.P., 2003. The effect of coloured noise on the uncertainties of rates estimated from geodetic time series, *Journal of Geodesy*, **76**, 483–494, doi: 10.1007/s00190-002-0283-4.
- Williams, S.D.P., Bock, Y., Fang, P., Jamason, P., Nikolaidis, R.M., Prawirodirdjo, L., Miller, M. & Johnson, D.J., 2004. Error analysis of continuous GPS position time series, *J. geophys. Res.*, **109**, B03412, doi:10.1029/2003JB002741.
- Zhang, J., Bock, Y., Johnson, H., Fang, P., Williams, S., Genrich, J., Wdowinski, S. & Behr, J., 1997. Southern California permanent GPS geodetic array: error analysis of daily position estimates and site velocities, *J. geophys. Res.*, **102**(B8), 18 035–18 055.